






A Phase I Dose-Escalation Study of the Pharmacokinetics, Pharmacodynamics, and Safety of a Single Oral Dose of Tigulixostat

Jun Tao ^{1,2,*}, Shuaibing Liu ^{1,2,*}, Ruijuan Liu ^{1,2}, Wenhua Xue ^{1,2}, Suke Sun¹, Suyun Wang¹, Chunjie Sun¹, Yidong Li¹, Chengzeng Wang³, Xin Tian ^{1,2}

¹Department of Pharmacy, The First Affiliated Hospital of Zhengzhou University, Zhengzhou, Henan, People's Republic of China; ²Henan Key Laboratory of Precision Clinical Pharmacy, The First Affiliated Hospital of Zhengzhou University, Zhengzhou, Henan, People's Republic of China; ³Henan Institute of Interconnected Intelligent Health Management, The First Affiliated Hospital of Zhengzhou University, Zhengzhou, Henan, People's Republic of China

*These authors contributed equally to this work

Correspondence: Xin Tian, Department of Pharmacy, The First Affiliated Hospital of Zhengzhou University, Zhengzhou, Henan, People's Republic of China, Tel +86-371-6629-5652, Email tianx@zzu.edu.cn

Aim: Tigulixostat is a promising selective xanthine oxidase inhibitor under clinical development for the treatment of hyperuricemia. The aim of this study was to evaluate the pharmacokinetics (PK), pharmacodynamics (PD), and safety of tigulixostat, along with its primary active metabolite, GD-MET-1, following single oral administration in healthy Chinese subjects.

Methods: A single center, open-label, dose-escalation study was conducted in healthy Chinese subjects who received single oral doses of tigulixostat ranging from 25 to 300 mg. Serial blood and urine samples were collected for PK and PD analysis. Safety was monitored throughout the study.

Results: Thirty subjects were enrolled, with six subjects per dose group. Tigulixostat exhibited dose-proportional increases in both maximum plasma concentration (C_{max}) and area under the concentration–time curve from time zero to infinity (AUC_{0-inf}), with coefficient of variation (CV%) for C_{max} ranging from 18.1% to 44.9% and for AUC_{0-inf} from 20.4% to 66.9%. The 24-hour mean serum uric acid decreased by 12.8% to 28.8% from baseline on Day 1, with greater reductions at higher doses. GD-MET-1 exposure increased with dose, with AUC_{0-inf} representing ~4.2–7.9% of parent exposure. Variability for GD-MET-1 was moderate (C_{max} CV%: 30.7%–43.5%; AUC_{0-inf} CV%: 24.8–38.9%). Tigulixostat demonstrated approximately dose-proportional PK, whereas GD-MET-1 showed less consistent proportionality, particularly for C_{max} . No serious adverse events occurred, and all treatment-emergent adverse events were mild in severity.

Conclusion: These findings demonstrate that tigulixostat exhibits approximately dose-proportional PK, with linear elimination and predictable exposure across the 25–300 mg range. A dose-dependent reduction in serum uric acid was observed up to 200 mg, with a plateau effect at 300 mg. The PK profile of GD-MET-1 indicated lower systemic exposure and less consistent dose proportionality compared with the parent compound, suggesting a supportive rather than dominant role in PD activity. The favorable safety and tolerability profile reinforces tigulixostat's potential as a novel therapeutic agent for the management of hyperuricemia.

Plain Language Summary:

What is already known about this subject

Xanthine oxidase inhibitors such as allopurinol and febuxostat are widely used for the treatment of hyperuricemia but may have limitations including hypersensitivity reactions, cardiovascular risk concerns, or limited efficacy in some patients.

Tigulixostat is a novel, selective xanthine oxidase inhibitor under clinical development, designed to offer improved safety and efficacy profiles.

There is limited data on the pharmacokinetics and pharmacodynamics of tigulixostat in Chinese populations.

What this study adds

This is the first study to characterize the pharmacokinetics, pharmacodynamics, and safety of tigulixostat in healthy Chinese subjects.

The drug demonstrated approximately dose-proportional exposure and a clear dose-dependent urate-lowering effect across a 25–300 mg dose range.

The pharmacokinetic profile of GD-MET-1 indicated lower systemic exposure and less consistent dose proportionality compared with the parent compound, suggesting a supportive rather than dominant role in pharmacodynamics activity.

Tigulixostat was well tolerated, with only mild adverse events observed.

Keywords: tigulixostat, GD-MET-1, xanthine oxidase inhibitor, hyperuricemia, dose escalation, pharmacokinetics, pharmacodynamics, safety

Introduction

Hyperuricemia, defined as elevated serum uric acid (sUA) levels, is a major pathogenic factor in gout and is increasingly associated with chronic kidney disease, hypertension, cardiovascular disease, and components of metabolic syndrome.^{1,2} The global prevalence of hyperuricemia has shown a rising trend over the past few decades. In the United States, it affects approximately 21.4% of men and 5.9% of women, while gout affects 3.9% of the population.³ In China, the estimated prevalence of hyperuricemia is approximately 13.3%, with a higher rate in males (19.4%) than in females (7.9%) and a national gout prevalence of around 1.1%.⁴ The rising incidence has increased the need for safer and more effective urate-lowering therapies.

Urate is primarily produced from the metabolism of readily absorbable dietary purines (such as guanine) or from the catabolism of endogenous purines, including adenosine triphosphate.⁵ Xanthine oxidase (XO) catalyzes the final two steps of purine catabolism, converting hypoxanthine to xanthine and subsequently to uric acid, the protonated form of urate.⁶ The main therapeutic approaches for hyperuricemia include XO inhibitors, which target this pathway to reduce sUA formation, and uricosuric agents that promote the renal excretion of sUA. Current XO inhibitors, including allopurinol and febuxostat, remain the first-line treatments for hyperuricemia and gout. However, the clinical limitations of currently approved XO inhibitors highlight an unmet need in specific patient populations. Allopurinol, although widely used, is primarily eliminated by the kidneys, requiring dose adjustment in patients with renal impairment.⁷ Moreover, allopurinol hypersensitivity syndrome, a rare but potentially fatal adverse reaction, is strongly associated with the HLA-B*58:01 allele. This allele is disproportionately prevalent in Asian populations, including Chinese, Thai, and Korean individuals, resulting in a significantly higher risk of severe cutaneous adverse reactions in these groups.^{8–11} Febuxostat has been linked to increased cardiovascular risk in patients.¹² Tigulixostat (Figure 1a) is a novel, potent, selective non-purine XO inhibitor developed to overcome these limitations.

Previous pharmacokinetic (PK) studies of tigulixostat in different ethnic populations are limited, with only one study conducted in healthy Korean subjects reporting its PK profiles. In that study, tigulixostat exhibited rapid absorption following oral administration, with a median time to maximum plasma concentration (T_{max}) of approximately 2–5 h and dose-proportional increases in systemic exposure over a dose range of 10–600 mg. The apparent clearance (CL/F) remained relatively consistent (~4–7 L/h), and the terminal half-life ($t_{1/2}$) ranged from ~5 to 15 h. Renal excretion fraction of unchanged drug was minimal (<0.4). Moreover, multiple-dose studies showed no clinically relevant drug accumulation (accumulation ratio ~1.1–1.3), suggesting stable PK at steady state.¹³ In a human mass balance study

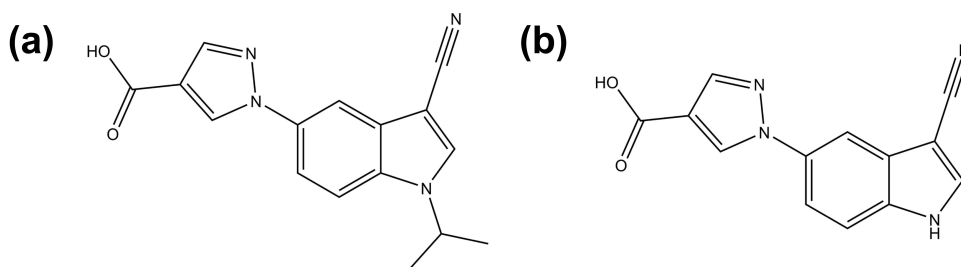


Figure 1 Chemical structure of tigulixostat (a) and its active metabolite GD-MET-1 (b).

following a single oral administration of [^{14}C]-tigulixostat (200 mg, 100 μCi), more than four metabolites were identified across biological matrices. Among them, M252/1 (GD-MET-1, [Figure 1b](#)), an N-dealkylated metabolite, was the most abundant, accounting for approximately 10% of total radioactivity exposure. In vitro studies showed that tigulixostat and GD-MET-1 inhibited XO with IC_{50} values of 0.003 and 0.002 μM in cow milk, and 0.073 and 0.069 μM in rat plasma, respectively. These inhibitory effects are comparable to those of febuxostat, which exhibited IC_{50} values of 0.002 μM in cow milk and 0.052 μM in rat plasma (Data on file).

Despite these promising pharmacological profiles, data on the PK, safety, and pharmacodynamics (PD) of tigulixostat in the Chinese population remain limited. Given potential inter-ethnic variability in drug metabolism, it is important to characterize tigulixostat's PK/PD properties in Chinese subjects. This study aimed to investigate the single-dose PK, urate-lowering efficacy, and safety of tigulixostat at doses ranging from 25 to 300 mg in healthy Chinese subjects. Additionally, the PK characteristics of GD-MET-1 were assessed to better understand its exposure profile and potential contribution to the overall pharmacological activity.

Materials and Methods

Ethics

The trial was conducted at the Phase I Clinical Research Center of The First Affiliated Hospital of Zhengzhou University. The protocol and informed consent form were approved by the Ethics Committee of Scientific Research and Clinical Trial, the First Affiliated Hospital of Zhengzhou University (approval number: L2023-Y368-002) and were implemented in accordance with the principles of the Declaration of Helsinki and the Good Clinical Practice guidelines. All participants signed written informed consent before undergoing any study-related procedures.

Subjects

Healthy subjects were recruited via public advertisements and hospital databases. Eligible participants were healthy male and female Chinese volunteers aged 18 to 50 years. At screening, male subjects were required to have a body weight ≥ 50 kg, and female subjects ≥ 45 kg, with a body mass index (BMI) between 18.0 and 28.0 kg/m^2 . All subjects were evaluated as healthy based on clinical laboratory tests, 12-lead electrocardiogram (ECG), vital signs, abdominal and urinary ultrasound, and physical examination, with any abnormalities deemed clinically insignificant by the investigator. Key exclusion criteria included a history of severe allergic reactions; any condition that might affect drug absorption or metabolism; clinically significant cardiovascular, hematologic, respiratory, endocrine, urologic, neurologic, or gastrointestinal diseases; history of psychiatric illness; use of prohibited concomitant medications within 30 days; prior participation in a tigulixostat study; history of gout flares; participation in other investigational studies within 30 days or 5 half-lives of a previous investigational product (whichever was longer); recent use (within 14 days) of any prescription or over-the-counter drugs, herbal supplements, or nutritional products (including vitamins); recent ingestion of grapefruit, Seville orange products, or caffeine/chocolate within 48 h; alcohol use >14 units/week or alcohol consumption within 48 h of admission; positive drug or alcohol screens; positive cotinine test indicating current smoking; significant blood donation or transfusion history; abnormal ECG findings (eg, corrected QT interval >450 ms); positive tests for hepatitis B, hepatitis C, HIV, or syphilis.

Laboratory exclusions included: alanine aminotransferase or aspartate aminotransferase values greater than the upper limit of normal (ULN); serum creatinine or urea nitrogen $>1.5 \times \text{ULN}$; abnormal thyroid function, defined as clinically significant changes in total triiodothyronine, total thyroxine, free triiodothyronine, free thyroxine, or thyroid-stimulating hormone levels; urinalysis indicating hematuria with clinical relevance; or sUA >480 $\mu\text{mol}/\text{L}$. Blood pressure outside the acceptable range (systolic ≤ 100 mmHg or ≥ 150 mmHg; diastolic ≤ 60 mmHg or ≥ 95 mmHg) after repeat measurement in a rested state also led to exclusion. Additionally, subjects were excluded if urinary ultrasound revealed kidney or bladder stones/crystals; if they were pregnant, lactating, or planning pregnancy within 3 months post-dose; if they had received vaccines within 3 months; had recent unprotected sexual activity (within 2 weeks); had personal or family history of malignancy; experienced any acute illness or concomitant medication use before dosing; had a history of needle phobia or difficulty with venipuncture; or were otherwise deemed unsuitable by the investigator. A total of 130 subjects were

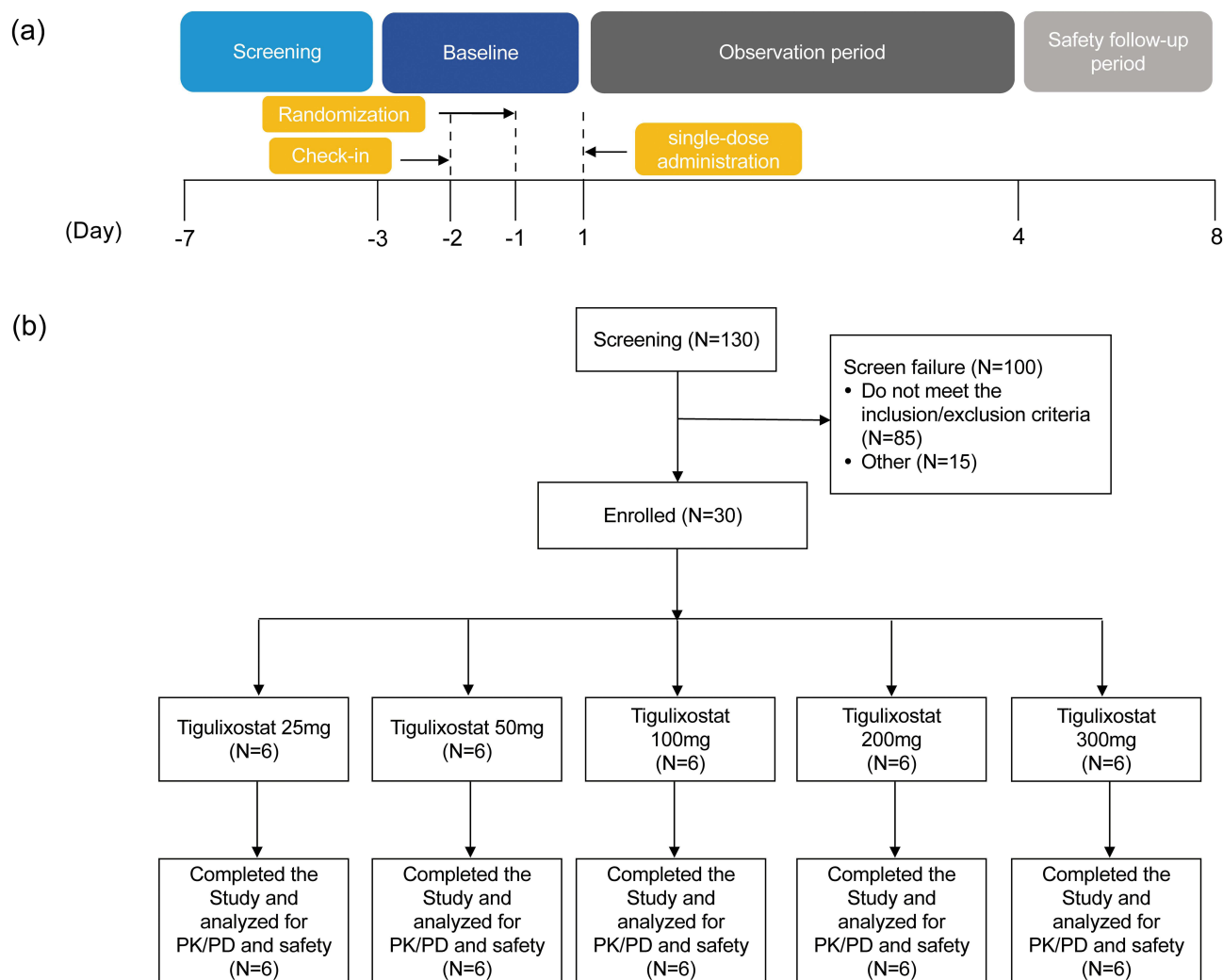


Figure 2 Flow diagrams of the current trial. Schematic of the trial duration (a) and schematic of the trial participants (b).

screened, of whom 30 were enrolled and 100 were excluded due to not meeting the inclusion/exclusion criteria (N=85) or other reasons (N=15).

Study Design and Procedures

This was a single-center, randomized, open-label, single-dose study conducted to investigate the PK, PD, and safety of tigulixostat in healthy Chinese adult subjects. Similar designs have been employed in recent biosimilar equivalence trials,¹⁴ ensuring robust evaluation of PK profiles. A total of 30 participants were enrolled and randomly assigned into five dose groups (25 mg, 50 mg, 100 mg, 200 mg, and 300 mg), with 6 subjects in each group. All participants received a single oral dose of tigulixostat under fasting conditions. The study design is illustrated in detail in the flowchart (Figure 2).

All subjects were admitted to the Phase I unit two days prior to dosing (Day -2) and remained in-house until at least 72 h post-dose for safety observation and sample collection. A follow-up safety visit was conducted 5–8 days after dosing. Blood samples for PK analysis of tigulixostat and GD-MET-1 were collected at the following time points: pre-dose (0 h), and 0.25, 0.5, 1, 1.5, 2, 2.5, 3, 3.5, 4, 5, 6, 8, 10, 12, 16, 24, 36, 48, and 72 h post-dose. After each blood sample was collected, the tube was gently inverted 8 to 10 times immediately to ensure proper mixing with the anticoagulant. The blood samples were then centrifuged at 4 °C, 1500 g for 10 minutes. The resulting plasma was carefully separated and temporarily stored at -70°C until analysis.

For PD evaluation of sUA, samples were obtained at -24, -18, and -12 h prior to dosing, within 1 h before administration on Day 1, and at 6, 12, 24, 48, and 72 h post-dose.

Bioanalytical Methods

Tigulixostat Quantification

Tigulixostat plasma concentrations were determined using a validated liquid chromatography-tandem mass spectrometry (LC-MS/MS) method with an API 6500 triple quadrupole mass spectrometer (Applied Biosystems/MDS Sciex, Foster City, CA). Chromatographic separation was achieved on a Phenomenex Luna C8 column (2.0 × 30 mm, 5.0 μm). The mobile phase consisted of 0.1% formic acid in water (A) and 0.1% formic acid in acetonitrile (B), with a flow rate of 0.35 mL/min. The gradient was programmed as follows: 0–0.2 min, 40% B; 0.2–0.9 min, linear increase to 80% B; 0.9–1.1 min, maintained at 80% B; 1.15–3.0 min, returned to 40% B. The internal standard was tigulixostat-d6. Detection was performed in positive ion mode using multiple reaction monitoring (MRM) with transitions of 295.0 → 235.0 for tigulixostat and 301.0 → 236.1 for the internal standard. The source voltage was 5500 V, curtain gas 30 psi, GS1 and GS2 both 50 psi, and ion source temperature was 500°C. The bioanalytical method for the determinations of tigulixostat concentrations in human plasma was validated in accordance with the United States Food and Drug Administration (FDA) Bioanalytical Method Validation Guidance and demonstrated good selectivity, linearity, precision, and stability. No significant endogenous interference was observed in six individual plasma lots, with peak areas <20% of the response at the lower limit of quantification (LLOQ), confirming adequate selectivity. The assay was linear over the concentration range of 10 ng/mL (LLOQ) to 10,000 ng/mL (upper limit of quantification, ULOQ) ($R^2 > 0.99$). Intra-batch precision was <3.8% at the LLOQ and <3.4% for other quality control levels, while inter-batch precision was <2.9% at the LLOQ and <2.8% for other concentrations. Tigulixostat showed good stability under various conditions: the stock solution was stable for 41 days, and the working solution for 78 days when stored in amber glass bottles in ethanol/water (1:1, v/v) at -70 °C. In plasma, it remained stable after five freeze-thaw cycles at -20 and -70°C, was stable for up to 83 days under long-term storage at the same temperatures, and processed samples were stable for 173 h in an autosampler at 6 °C.

GD-MET-1 Quantification

The plasma concentration of GD-MET-1 was determined using an API 5500 mass spectrometer (Applied Biosystems/MDS Sciex, Foster City, CA) with chromatographic separation on an Imtakt Cadenza CD-C18 column (2.1 × 150 mm, 3.0 μm). The mobile phase A was 0.1% formic acid in water, and mobile phase B was a mixture of acetonitrile and methanol (3:2, v/v) containing 0.1% formic acid. The flow rate was 0.4 mL/min. The gradient program was as follows: 0.01–3.0 min, 45%–60% B; 3.0–3.5 min, increased to 90% B; 3.5–4.4 min, held at 90% B; 4.5–5.5 min, returned and held at 45% B. The internal standard was $^{13}\text{C}_3$ -GD-MET-1. Detection was performed in negative ion mode with MRM transitions of 251.1 → 166.0 for GD-MET-1 and 254.0 → 166.0 for the internal standard. The source voltage was -4500 V, curtain gas 30 psi, GS1 and GS2 both 50 psi, and source temperature 500 °C. The bioanalytical method for the determination of plasma GD-MET-1 concentrations in human plasma was also validated according to the FDA Bioanalytical Method Validation Guidance and met all acceptance criteria. The assay demonstrated good selectivity, with no significant endogenous interference observed in six individual plasma lots, and peak areas <20% of the LLOQ response. Linearity was confirmed over the concentration range of 5 ng/mL (LLOQ) to 2000 ng/mL (ULOQ) ($R^2 > 0.99$). Intra-batch precision was <6.9% at the LLOQ and <4.9% for other quality control levels, while inter-batch precision was <5.1% at the LLOQ and <3.7% for other levels. GD-MET-1 also exhibited acceptable stability under various conditions. The stock solution was stable for 47 days, and the working solution for 62 days when stored in amber glass bottles in dimethyl sulfoxide at -70 °C. In plasma, it was stable after five freeze-thaw cycles at -20 and -70 °C, remained stable for up to 72 days under long-term storage at the same temperatures, and processed samples were stable for 176 h in an autosampler at 6 °C.

sUA Quantification

The sUA concentration was measured using an enzymatic colorimetric method. In this assay, uricase catalyzes the oxidation of uric acid to allantoin and hydrogen peroxide. The generated hydrogen peroxide then reacts with

4-aminophenazone and N-ethyl-N-(2-hydroxy-3-sulfoxypropyl)-3-methylaniline in the presence of peroxidase to form a red quinone-diimine dye. The intensity of the resulting color, which is directly proportional to the uric acid concentration, was quantified by measuring the absorbance.

PK and PD Analysis

PK parameters were calculated using non-compartmental analysis (NCA) with PKanalix (version 2023R1, Lixoft, France). The maximum observed plasma concentration (C_{\max}) and time to reach C_{\max} (T_{\max}) were obtained directly from the concentration-time data. The area under the plasma concentration-time curve from time zero to the last quantifiable concentration ($AUC_{0-\text{last}}$) was calculated using the linear trapezoidal rule. The area under the curve extrapolated to infinity ($AUC_{0-\text{inf}}$) was estimated as $AUC_{0-\text{last}}$ plus the last measured concentration divided by the terminal elimination rate constant (λ_z), which was derived from the log-linear terminal phase. The $t_{1/2}$ was calculated as $\ln(2)/\lambda_z$. CL/F was calculated as $\text{dose}/AUC_{0-\text{inf}}$, and apparent volume of distribution (V/F) was calculated as CL/F divided by λ_z .

PD parameters included the 24-h mean sUA concentration ($C_{\text{mean},24}$) and the area under the concentration-time curve from 0 to 24 h (AUC_{0-24}). AUC_{0-24} was calculated using the linear trapezoidal method, and $C_{\text{mean},24}$ was derived as AUC_{0-24} divided by 24. Changes in $C_{\text{mean},24}$ were expressed as percentage reductions from baseline.

Statistical Analysis

Statistical analyses were performed using SPSS[®] software, version 21.0 (SPSS Inc., Chicago, IL, USA). Descriptive statistics were applied to summarize PK and PD parameters across dose groups. Continuous variables were reported as mean, standard deviation (SD), and coefficient of variation (CV%). T_{\max} , which is typically not normally distributed, was summarized using the median, minimum, and maximum values. In cases where only descriptive summaries were intended, no formal hypothesis testing was performed.

Dose proportionality of tigulixostat and GD-MET-1 was evaluated using the power model, implemented in GraphPad Prism, version 8.0 (GraphPad Software, LLC, San Diego, CA, USA). PK parameters (C_{\max} , $AUC_{0-\text{inf}}$, and CL/F) for each subject were log-transformed and analyzed according to the regression model (Equation 1):

$$\ln(\text{PKparameter}) = \beta \cdot \ln(\text{Dose}) + \alpha$$

where β is the slope and α is the intercept. A β of 1 indicates perfect dose proportionality. To assess approximate proportionality, the predefined equivalence interval was set at 0.90–1.10, such that if the 95% confidence interval (CI) of β was entirely within this range, dose proportionality was concluded. Statistical significance of the regression slope was evaluated using an *F*-test, and coefficients of determination (R^2) were reported.

Safety Assessment

The safety evaluation in this study involved continuous monitoring of adverse events (AEs) and serious adverse events (SAEs) from the initial dose through the safety follow-up period. Safety assessments also included vital signs, physical examinations, 12-lead ECGs, and a range of clinical laboratory tests, such as hematology, serum biochemistry, and urinalysis, along with abdominal and urinary system ultrasounds and thyroid function evaluations.

Results

Subject Demographics

A total of 30 subjects were enrolled in the study, with 6 participants assigned to each dose group. The mean (\pm SD) age of participants ranged from 30.7 to 35.5 years across the five dose groups. The sex distribution was generally balanced, with 50.0–66.7% male and 33.3–50.0% female in each group. Mean height ranged from 165 to 169 cm, and mean body weight ranged from 60.7 to 68.5 kg. BMI values were within the normal range for all groups, with mean BMI ranging from 22.1 to 24.6 kg/m². The demographic characteristics were generally comparable across dose groups, indicating a well-balanced study population (Table 1).

Table 1 Demographic and Baseline Characteristics

	25 mg (N=6)	50 mg (N=6)	100 mg (N=6)	200 mg (N=6)	300 mg (N=6)
Age (years)					
Mean (SD)	30.8 (7.63)	31.2 (7.39)	32.0 (11.21)	30.7 (5.82)	35.5 (8.09)
Sex, n (%)					
Male	4 (66.7)	4 (66.7)	4 (66.7)	4 (66.7)	3 (50.0)
Female	2 (33.3)	2 (33.3)	2 (33.3)	2 (33.3)	3 (50.0)
Height (cm)					
Mean (SD)	166 (10.7)	169 (9.36)	166 (9.68)	167 (8.04)	165 (6.55)
Body weight (kg)					
Mean (SD)	63.2 (7.01)	65.4 (11.9)	60.7 (6.42)	68.5 (7.74)	61.6 (6.14)
BMI (kg/m ²)					
Mean (SD)	22.8 (1.17)	22.7 (2.42)	22.1 (2.31)	24.6 (1.60)	22.7 (2.89)

Abbreviations: SD, standard deviation; BMI, Body mass index.

PK of Tigulixostat and GD-MET-1

Following single oral administration of tigulixostat at doses ranging from 25 mg to 300 mg in healthy Chinese subjects, tigulixostat was rapidly absorbed, with median T_{max} values ranging from 2.75 to 4.01 h across dose groups. The plasma concentration-time profile exhibited a biphasic decline, and both C_{max} and AUC_{0-inf} increased in a dose-proportional manner (Figure 3a and Table 2). The mean terminal elimination half-life ($t_{1/2}$) ranged from 7.26 to 10.2 h. Moderate inter-individual variability was observed for tigulixostat PK. The PK parameters of tigulixostat for each subject are provided in [Supplementary Table S1](#). The CV% for C_{max} ranged from 18.1% to 44.9%, while that for AUC_{0-inf} ranged from 20.4% to 66.9%, with notably higher variability at the 50 mg and 200 mg dose levels. This variability may reflect differences in absorption, metabolism, or other physiological factors.

GD-MET-1, the major circulating active metabolite of tigulixostat, showed a similar T_{max} (3.00–4.51 h) and a shorter $t_{1/2}$ (2.00–7.64 h) compared to the parent compound. [Supplementary Table S2](#) contains the PK parameters of GD-MET-1 for each subject. Its systemic exposure was substantially lower, with AUC_{0-inf} values accounting for approximately 4.20% to 7.90% of tigulixostat across dose levels. GD-MET-1 also exhibited moderate variability, with CV% for C_{max} ranging from 30.7% to 43.5% and for AUC_{0-inf} from 24.8% to 38.9% (Figure 3b and Table 2). These findings suggest that while GD-MET-1 may contribute to the pharmacodynamic effect, it likely plays a supportive rather than dominant role.

To further assess the dose proportionality of tigulixostat and GD-MET-1, a power model analysis was performed. For tigulixostat, the slope (β) for C_{max} was 1.038 (95% confidence interval [CI] for slope: 0.912–1.164, $R^2 = 0.910$, $p <$

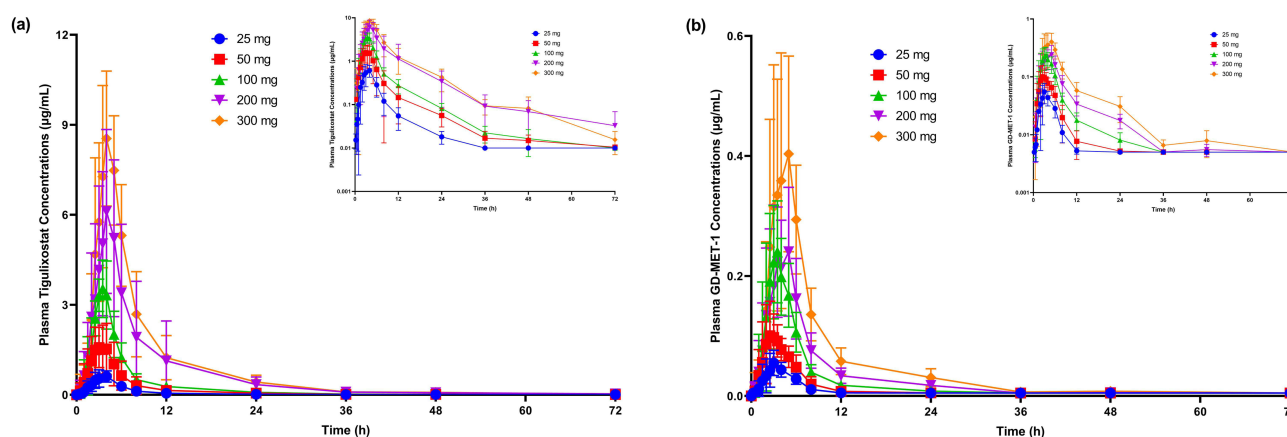


Figure 3 Mean plasma concentration-time profiles of tigulixostat (a) and its active metabolite GD-MET-1 (b) following single oral doses of 25 mg, 50 mg, 100 mg, 200 mg and 300 mg in healthy subjects. Data are presented as mean \pm standard deviation. The upper-right insets show the same data plotted on a semi-logarithmic scale to better visualize the elimination phase.

Table 2 The Pharmacokinetic Parameters (Mean±SD, CV%) for Tigulixostat and Its Primary Active Metabolite, GD-MET-1 After Single Oral Doses of 25, 50, 100, 200, and 300 mg

Analytes	Dose (mg)	N	C _{max} (µg/mL)	T _{max} (h)	t _{1/2} (h)	AUC _{0-last} (µg h/mL)	AUC _{0-inf} (µg h/mL)	CL/F (L/h)	V/F (L)
Tigulixostat	25	6	0.672±0.178 (26.5%)	3.26 (2.48,4.02)	7.26±4.84 (66.7%)	3.26±0.838 (25.7%)	3.45±0.796 (23.1%)	7.55±1.59 (21.1%)	83.5±70.6 (84.5%)
	50	6	1.89±0.848 (44.9%)	2.75 (1.50,4.00)	11.3±10.1 (89.2%)	9.35±4.99 (53.4%)	9.63±5.11 (53.0%)	6.28±2.61 (41.6%)	80.9±31.5 (39.0%)
	100	6	3.70±0.848 (22.9%)	2.99 (2.98,4.00)	7.89±1.94 (66.7%)	17.0±3.45 (20.2%)	17.2±3.51 (20.4%)	6.01±1.23 (20.5%)	68.4±23.1 (33.8%)
	200	6	6.64±2.06 (31.1%)	4.01 (3.00,5.00)	10.2±3.17 (31.1%)	42.9±28.9 (67.5%)	43.6±29.2 (66.9%)	6.13±3.36 (54.8%)	91.8±57.5 (62.6%)
	300	6	9.19±1.66 (18.1%)	4.01 (4.00,5.07)	8.34±2.19 (26.2%)	55.9±17.9 (32.0%)	56.3±17.9 (31.9%)	5.71±1.49 (26.0%)	69.7±30.3 (43.5%)
GD-MET-1	25	6	0.0553±0.0211 (38.1%)	3.00 (2.00,5.98)	2.07±0.462 (22.3%)	0.222±0.091 (40.7%)	0.273±0.0846 (31.0%)	98.3±27.5 (28.0%)	291±86.7 (29.8%)
	50	6	0.116±0.0445 (38.3%)	2.50 (2.00,5.00)	3.23±1.29 (39.9%)	0.525±0.210 (40.1%)	0.558±0.217 (38.9%)	105.2±49.1 (46.6%)	431±134 (31.1%)
	100	6	0.247±0.0877 (35.5%)	3.24 (2.50,3.52)	6.73±2.36 (35.0%)	1.21±0.438 (36.1%)	1.29±0.441 (34.2%)	86.2±32.8 (38.0%)	893±606 (67.9%)
	200	6	0.288±0.0885 (30.7%)	4.25 (3.00,5.00)	7.64±2.68 (35.1%)	1.67±0.246 (25.5%)	1.82±0.452 (24.8%)	115.5±28.2 (24.4%)	1351±766 (56.7%)
	300	6	0.420±0.183 (43.5%)	4.51 (3.00,5.07)	6.89±1.78 (25.8%)	2.89±0.796 (27.5%)	2.99±0.834 (27.9%)	106.8±28.4 (26.6%)	1074±380 (35.4%)

Abbreviations: SD, standard deviation; CV, coefficient of variation; N, number; C_{max}, maximum plasma drug concentration; t_{1/2}, elimination half-life; h, hours; T_{max}, time to reach peak plasma drug concentrations; AUC_{0-last}, area under the plasma concentration–time curve (AUC) from 0 h to 72 h; AUC_{0-inf}, AUC from time zero to infinity; CL/F, apparent total clearance of the drug from plasma after oral administration; V/F, apparent volume of distribution.

0.0001, Figure 4a), and the slope for AUC_{0-inf} was 1.106 (95% CI: 0.951–1.261, R² = 0.884, *p* < 0.0001, Figure 4b). Both estimates fell within the predefined equivalence interval ($\beta = 1.0 \pm 0.1$; ie, 0.90–1.10), confirming dose-proportional increases in exposure, although AUC_{0-inf} approached the upper bound. In contrast, the slope for apparent oral clearance (CL/F) was –0.106 (95% CI: –0.261 to 0.049, R² = 0.066, *p* = 0.172, Figure 4c), indicating dose-independent clearance.

For GD-MET-1, the slope for C_{max} was 0.786 (95% CI: 0.632–0.939, R² = 0.797, *p* < 0.0001, Figure 4d), which was below the equivalence interval, suggesting less than dose-proportional increases. The slope for AUC_{0-inf} was 0.947 (95% CI: 0.804–1.089, R² = 0.873, *p* < 0.0001, Figure 4e), supporting approximate dose proportionality. The slope for CL/F was 0.053 (95% CI: –0.089 to 0.196, R² = 0.021, *p* = 0.449, Figure 4f), further confirming clearance was independent of dose.

PD

Mean sUA concentration-time profiles stratified by dose are shown in Figure 5. After dosing, sUA levels declined gradually. In the 25, 50, and 100 mg groups, the lowest mean sUA concentrations were observed around 12 h post-dose, followed by a slow recovery. In contrast, sUA concentrations in the 200 and 300 mg groups continued to decline through 24 h. The PD parameters of sUA for each subject are provided in Supplementary Table S3.

On Day 1 post-dose, the estimated C_{mean,24} decreased from baseline by 12.8% to 28.8% across groups. Specifically, the mean percentage reductions in C_{mean,24} were 12.8%, 15.7%, 23.7%, 28.8%, and 26.4% for the 25, 50, 100, 200, and 300 mg groups, respectively (Table 3). The extent of sUA reduction increased with dose up to 200 mg, beyond which the effect plateaued. For AUC₀₋₂₄, baseline values ranged from 114 mg·h/dL in the 25 mg group to 108 mg·h/dL in the 300 mg group. On Day 1, reductions in AUC₀₋₂₄ mirrored those of C_{mean,24}, with decreases of 12.8%, 15.7%, 23.7%, 28.8%, and 26.4% corresponding to the respective doses (Table 3). The greatest reductions in both AUC₀₋₂₄ and C_{mean,24} were observed in the 200 mg and 300 mg dose groups, indicating a clear dose-response relationship in tigulixostat's urate-lowering effect.

Safety

In this study, the incidence of treatment-emergent adverse events (TEAEs) across the five dose groups (25 mg, 50 mg, 100 mg, 200 mg, and 300 mg) is summarized in Table 4. The incidence of TEAEs was 16.7% in the 25 mg group (1 subject), 50.0% in the 50 mg group (3 subjects), 33.3% in the 100 mg group (2 subjects), 33.3% in the 200 mg group (2 subjects), and 16.7% in the 300 mg group (1 subject). The overall incidence of TEAEs across all groups was 30.0% (9 subjects). The most reported TEAEs, classified by System Organ Class, were laboratory tests (16.7% of cases). By Preferred Term, the TEAEs occurring in at least two subjects included hypertriglyceridemia (10.0%), decreased neutrophil count (6.70%), and decreased leukocyte count (6.70%). Other AEs such as transient increased blood pressure, heart rate, and urinary abnormalities were not observed in more than one subject across the groups. Importantly, all

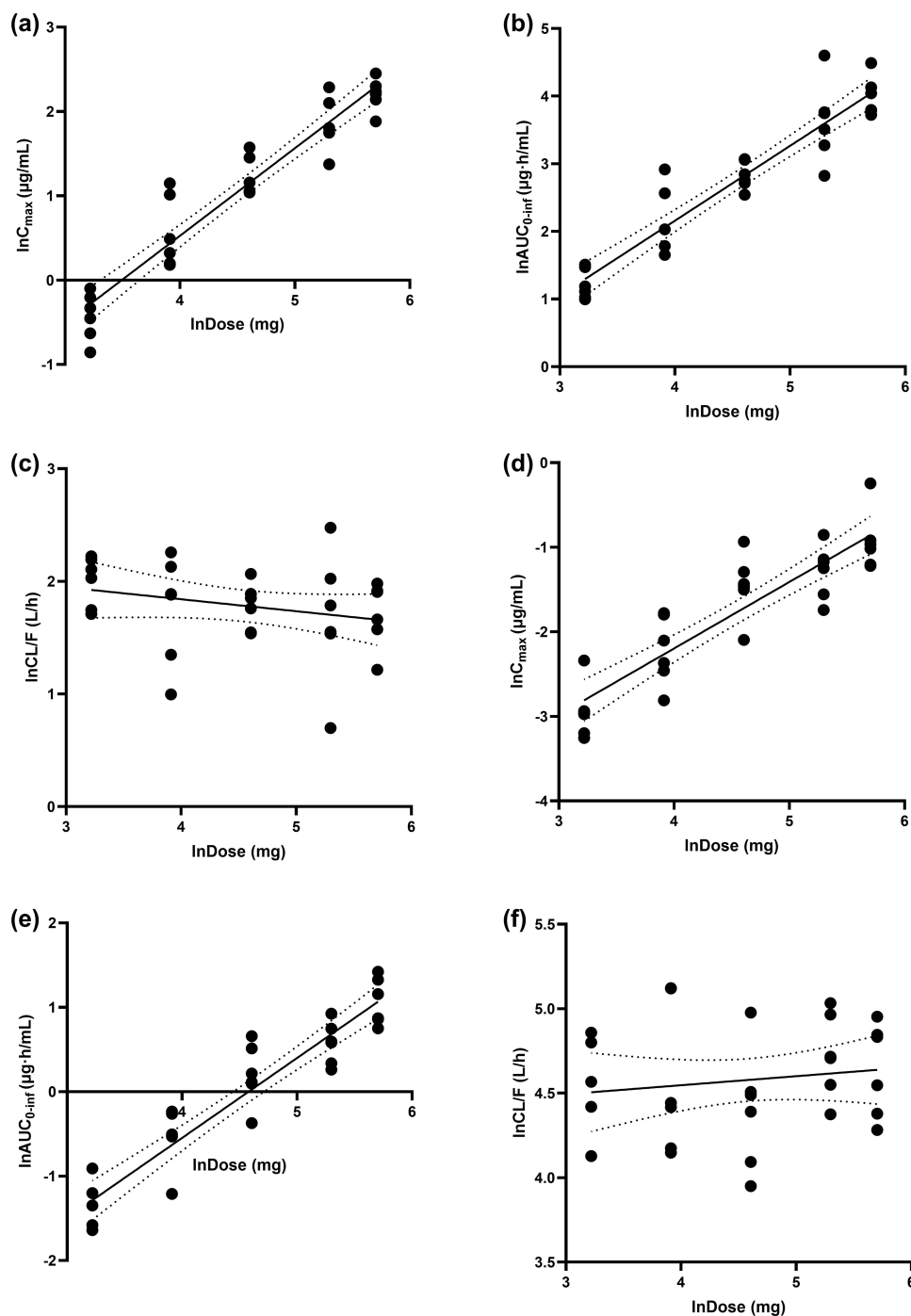


Figure 4 Correlation between tiglixostat dose and pharmacokinetic parameters of tiglixostat and its active metabolite GD-MET-I. (a) C_{max} , (b) AUC_{0-inf} , and (c) apparent oral clearance (CL/F) of tiglixostat; (d) C_{max} , (e) AUC_{0-inf} , and (f) CL/F of GD-MET-I are plotted across the 25–300 mg dose range. Each black dot represents an individual subject; dashed lines indicate group mean errors; and solid black lines represent log-log power model regression fits. The regression equations, slopes (β) with 95% confidence intervals (CI), coefficients of determination (R^2), and p values were as follows, with the equivalence interval for dose proportionality predefined as $\beta = 1.0 \pm 0.1$ (0.90–1.10): (a) $\ln(C_{max}) = 1.038 \cdot \ln(\text{Dose}) - 3.624$, $\beta = 1.038$ (95% CI: 0.912–1.164), $R^2 = 0.910$, $p < 0.0001$; (b) $\ln(AUC_{0-inf}) = 1.106 \cdot \ln(\text{Dose}) - 2.266$, $\beta = 1.106$ (95% CI: 0.951–1.261), $R^2 = 0.884$, $p < 0.0001$; (c) $\ln(\text{CL}/F) = -0.106 \cdot \ln(\text{Dose}) + 2.266$, $\beta = -0.106$ (95% CI: -0.261–0.049), $R^2 = 0.066$, $p = 0.172$; (d) $\ln(C_{max}) = 0.786 \cdot \ln(\text{Dose}) - 5.339$, $\beta = 0.786$ (95% CI: 0.632–0.939), $R^2 = 0.797$, $p < 0.0001$; (e) $\ln(AUC_{0-inf}) = 0.947 \cdot \ln(\text{Dose}) - 4.333$, $\beta = 0.947$ (95% CI: 0.804–1.089), $R^2 = 0.873$, $p < 0.0001$; (f) $\ln(\text{CL}/F) = 0.053 \cdot \ln(\text{Dose}) + 4.333$, $\beta = 0.053$ (95% CI: -0.089–0.196), $R^2 = 0.021$, $p = 0.449$.

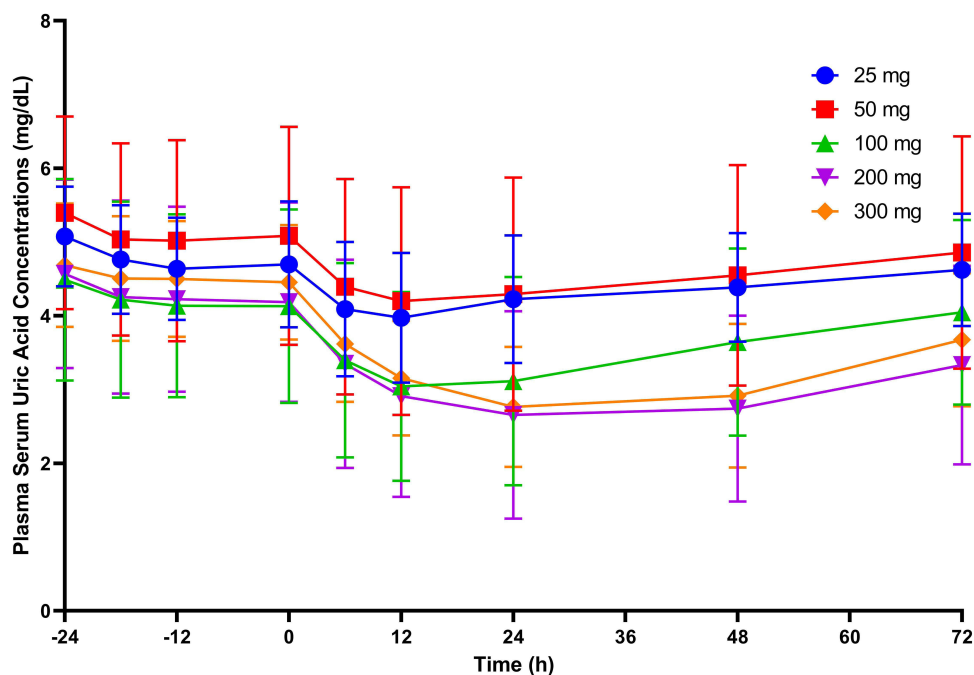


Figure 5 Serum uric acid concentration-time profiles following single oral administration of tiglixostat at 25 mg, 50 mg, 100 mg, 200 mg, and 300 mg in healthy Chinese subjects.

TEAEs were of mild severity, resolved spontaneously without medical intervention. There were no SAEs, and no new safety concerns were identified.

Discussion

This study systematically characterized the PK, PD, and safety of tiglixostat, a novel selective XO inhibitor, following single oral administration at doses ranging from 25 to 300 mg in healthy Chinese subjects. Tiglixostat was rapidly absorbed, with a median T_{max} of approximately 2.75 to 4.01 h across all dose levels. Systemic exposure, represented by C_{max} and AUC, increased in an approximately dose-proportional manner, supporting the conclusion that tiglixostat exhibits linear PK within the studied range. Apparent CL/F remained relatively stable across doses, further confirming the linearity of tiglixostat disposition in healthy Chinese subjects. These results are consistent with findings from previous studies in healthy Korean subjects, including dose-proportional increases in exposure and comparable $t_{1/2}$.¹³ The interethnic similarity suggests that tiglixostat's PK are not significantly influenced by Chinese and Korean populations. Further investigations into sex-specific pharmacokinetics, as demonstrated in studies of other compounds like kokusaginine,¹⁵ may provide additional insights into tiglixostat's variability. Additionally, future studies could explore

Table 3 The Pharmacodynamic Parameters (Mean \pm SD, CV%) Following Single Oral Administration of Tiglixostat at 25 mg, 50 mg, 100 mg, 200 mg, and 300 mg

Dose (mg)	N	$C_{mean,24}$ (mg/dL)		Change in $C_{mean,24}$ (%)	AUC ₀₋₂₄ (mg h/dL)		Change in AUC ₀₋₂₄ (%)
		Baseline	Day I		Baseline	Day I	
25	6	4.74 \pm 0.731 (15.4%)	4.16 \pm 0.883 (21.2%)	12.8 \pm 5.75 (45.0%)	113.7 \pm 17.6 (15.4%)	99.9 \pm 21.2 (21.2%)	12.8 \pm 5.75 (45.0%)
50	6	5.09 \pm 1.37 (26.9%)	4.39 \pm 1.53 (34.7%)	15.7 \pm 9.11 (58.2%)	122.1 \pm 32.9 (26.9%)	105 \pm 36.6 (34.7%)	15.7 \pm 9.11 (58.2%)
100	6	4.20 \pm 1.29 (30.8%)	3.29 \pm 1.32 (40.2%)	23.7 \pm 9.35 (39.4%)	100.8 \pm 31.0 (30.8%)	79.1 \pm 31.8 (40.2%)	23.7 \pm 9.35 (39.4%)
200	6	4.26 \pm 1.29 (30.3%)	3.13 \pm 1.39 (44.4%)	28.8 \pm 10.9 (37.8%)	102.2 \pm 31.0 (30.3%)	75.1 \pm 33.4 (44.4%)	28.8 \pm 10.9 (37.8%)
300	6	4.51 \pm 0.799 (17.7%)	3.35 \pm 0.786 (23.5%)	26.4 \pm 5.41 (20.5%)	108.2 \pm 19.2 (17.7%)	80.3 \pm 18.9 (23.5%)	26.4 \pm 5.41 (20.5%)

Abbreviations: SD, standard deviation; CV, coefficient of variation; h, hours; $C_{mean,24}$, 24-h mean serum concentrations of uric acid; AUC₀₋₂₄, area under the serum uric acid concentration-time curve (AUC) from 0 h to 24 h.

Table 4 Summary of Treatment-Emergent Adverse Events (TEAE) by System Organ Class and Preferred Term Across Five Tiglixostat Dose Groups. Values Represent the Number and Percentage of Subjects (N = 6 per Group) Reporting at Least One TEAE

Preferred System Organ Class Preferred Term n (%)	25 mg (N=6)	50 mg (N=6)	100 mg (N=6)	200 mg (N=6)	300 mg (N=6)	Summary (N=30)
At least 1 occurrence of TEAE	1 (16.7)	3 (50.0)	2 (33.3)	2 (33.3)	1 (16.7)	9 (30.0)
Laboratory tests						
Decreased neutrophil count	1 (16.7)	1 (16.7)	0	0	0	2 (6.70)
Decreased white blood cell count	1 (16.7)	1 (16.7)	0	0	0	2 (6.70)
Positive urine leukocytes	0	0	0	1 (16.7)	0	1 (3.30)
Increased heart rate	0	0	1 (16.7)	0	0	1 (3.30)
Elevated blood pressure	0	0	1 (16.7)	0	0	1 (3.30)
Metabolic and nutritional disorders						
Hypertriglyceridemia	0	2 (33.3)	0	0	1 (16.7)	3 (10.0)
Infections and infestations						
Upper respiratory tract infection	0	0	0	1 (16.7)	0	1 (3.30)

advanced delivery systems, such as polyethylene glycol–phosphatidylethanolamine micelles, to further optimize its PK behavior and reduce variability, as demonstrated with other therapeutics.¹⁶

A significant strength of the present study lies in the simultaneous evaluation of GD-MET-1, the major active metabolite of tiglixostat. GD-MET-1 exhibited measurable systemic exposure that increased with dose, though its $t_{1/2}$ was shorter and clearance higher than that of the parent compound. Greater inter-individual variability in GD-MET-1 C_{max} was observed, particularly at higher doses. Although the underlying mechanisms remain unclear, several factors may contribute. Genetic polymorphisms in drug-metabolizing enzymes mediating GD-MET-1 formation could play a role. Dietary factors, including purine-rich food intake, could also influence endogenous XO activity and indirectly alter metabolite exposure. Additionally, unmeasured covariates such as gut microbiota composition or inter-individual differences in hepatic blood flow at higher oral doses may also contribute. These hypotheses warrant further investigation in larger, ethnically diverse populations. While GD-MET-1 likely contributes to the overall urate-lowering effect, its transient exposure suggests it plays a supportive rather than dominant role. Further studies involving repeated dosing and PK/PD modeling are warranted to quantify its contribution more precisely.

Dose proportionality analysis confirmed the linear PK behavior of tiglixostat across the studied dose range. Both C_{max} and AUC_{0-inf} exhibited slopes close to unity, with 95% CI contained within the predefined equivalence interval (0.90–1.10), supporting dose proportionality and predictable systemic exposure. This linearity is consistent with the observed dose-dependent reductions in serum uric acid, further underscoring tiglixostat as the primary driver of urate-lowering efficacy. These findings are consistent with previous results reported in healthy Korean subjects.¹³ In contrast, the active metabolite GD-MET-1, showed lower systemic exposure (AUC_{0-inf} approximately 4.20–7.90% of parent compound) and a shorter half-life (2.00–7.64 h), coupled with less consistent dose proportionality as its slopes deviated from the equivalence interval. The less-than-dose-proportional increase in C_{max} for GD-MET-1 may be attributed to a formation-limited process, where metabolic conversion of tiglixostat becomes saturated at higher doses. Additionally, the higher inter-individual variability in C_{max} supports this explanation, suggesting that differences in hepatic enzyme activity or hepatic blood flow may influence metabolite formation. Given its substantially lower systemic exposure and short half-life, this deviation is unlikely to have clinical relevance. Overall, these findings suggest that GD-MET-1 contributes only modestly to the overall PD effect, playing a supportive rather than dominant role in the urate-lowering activity of tiglixostat.

From a PD perspective, sUA levels declined in a dose-dependent manner, with $C_{mean,24}$ decreasing by up to 28.8% after a single dose. A plateauing trend between the 200 mg and 300 mg groups indicates a potential ceiling effect in XO inhibition. This aligns with the known pharmacologic limits of XO inhibition, where additional dose increases yield minimal further reduction in sUA.⁷ These findings have important implications for dose optimization. Considering the balance between efficacy and safety, 200 mg may represent a clinically meaningful upper threshold for further evaluation

in Phase II/III trials. It could serve as the highest target dose in future studies, achieving maximal urate-lowering efficacy while avoiding unnecessary high exposure.

Compared to existing XO inhibitors such as febuxostat and allopurinol, tigulixostat exhibits a favorable PK profile, particularly with regard to its predictable linear kinetics and consistent urate-lowering effects. Allopurinol, despite its widespread use, has limitations due to its short $t_{1/2}$ and heavy dependence on renal clearance. The side effects of allopurinol, although uncommon, may be severe or life-threatening and occur more often in patients with renal insufficiency, limiting its use in patients with renal impairment.^{17,18} Febuxostat, although more potent, has raised cardiovascular safety concerns in some populations.¹² Tigulixostat, with its predictable PK profile may offer a better alternative. However, head-to-head comparisons and long-term studies are required to validate these potential benefits.

The safety profile observed in this study was favorable. Overall, the incidence of TEAEs was low, with hypertriglyceridemia (10.0%) being the most common TEAE. This finding warrants careful monitoring in patients with hyperuricemia or gout, who often have comorbid metabolic syndrome or cardiovascular risk factors, as elevated triglyceride levels could potentially exacerbate underlying conditions. The underlying mechanism remains unclear but may involve alterations in lipid metabolism secondary to XO inhibition, as XO has been implicated in oxidative stress pathways affecting lipid homeostasis.¹⁹ Further mechanistic studies are required to confirm whether this effect is drug-related or incidental in healthy subjects. No SAEs or discontinuations due to AEs were reported.

One limitation of this study was conducted in healthy subjects, so PK/PD in patients with hepatic or biliary dysfunction (eg, post-biliary drainage) remains unknown. Biliary excretion has been shown to critically modulate drug PK,²⁰ warranting further tigulixostat studies in such populations. Additionally, as this was a single-dose study, multiple-dose regimens need to be evaluated to assess drug accumulation and steady-state PK. Future studies should also investigate the effects of food intake and renal impairment, as these factors may further influence PK and PD characteristics of tigulixostat. Another consideration is that the specific metabolic enzymes responsible for tigulixostat biotransformation have not yet been definitively identified. As a result, we were unable to assess the impact of genetic polymorphisms or potential drug-drug interactions involving metabolic enzyme inhibitors or inducers.²¹ It is an important area for future research to better understand inter-individual variability and safety risks. Ongoing work by our group is focused on identifying the relevant metabolic pathways of tigulixostat.

Conclusion

In summary, these findings demonstrate that tigulixostat exhibits approximately dose-proportional PK, with linear elimination and predictable exposure across the 25–300 mg range. A dose-dependent reduction in serum uric acid was observed up to 200 mg, with a plateau effect at 300 mg. The PK profile of GD-MET-1 indicated lower systemic exposure and less consistent dose proportionality compared with the parent compound, suggesting a supportive rather than dominant role in PD activity. The favorable safety and tolerability profile reinforces tigulixostat's potential as a novel therapeutic agent for the management of hyperuricemia.

Clinical Trial Registration

NCT06277752 (ClinicalTrials.gov); registered on 4 February 2024.

Data Sharing Statement

The data that support the findings of this study are available from the corresponding author, Xin Tian, upon reasonable request.

Acknowledgments

We thank all study participants for their invaluable contributions.

Author Contributions

All authors made a significant contribution to the work reported, whether that is in the conception, study design, execution, acquisition of data, analysis and interpretation, or in all these areas; took part in drafting, revising or critically

reviewing the article; gave final approval of the version to be published; have agreed on the journal to which the article has been submitted; and agree to be accountable for all aspects of the work.

Funding

This study was funded by Innovent Biologics (Suzhou) Co., Ltd. The sponsor was involved in the study design, conduct of the study, and financial support, but had no role in data analysis, interpretation, or preparation of this paper.

Disclosure

The sponsor's role was limited to funding, study design, and conduct of the study, and the authors declare no other conflicts of interest.

References

1. Richette P, Doherty M, Pascual E, et al. 2016 updated EULAR evidence-based recommendations for the management of gout. *Ann Rheum Dis.* 2017;76(1):29–42. doi:10.1136/annrheumdis-2016-209707
2. Johnson RJ, Nakagawa T, Jalal D, et al. Uric acid and chronic kidney disease: which is chasing which? *Nephrol Dial Transplant.* 2013;28(9):2221–2228. doi:10.1093/ndt/gft029
3. Zhu Y, Pandya BJ, Choi HK. Prevalence of gout and hyperuricemia in the US general population: the national health and nutrition examination survey 2007–2008. *Arthritis Rheum.* 2011;63(10):3136–3141. doi:10.1002/art.30520
4. Liu R, Han C, Wu D, et al. Prevalence of hyperuricemia and gout in Mainland China from 2000 to 2014: a systematic review and meta-analysis. *Biomed Res Int.* 2015;2015:762820. doi:10.1155/2015/762820
5. Hyndman D, Liu S, Miner JN. Urate handling in the human body. *Curr Rheumatol Rep.* 2016;18(6):34. doi:10.1007/s11926-016-0587-7
6. Martillo MA, Nazzal L, Crittenden DB. The crystallization of monosodium urate. *Curr Rheumatol Rep.* 2014;16(2):400. doi:10.1007/s11926-013-0400-9
7. Day RO, Graham GG, Hicks M, et al. Clinical pharmacokinetics and pharmacodynamics of allopurinol and oxypurinol. *Clin Pharmacokinet.* 2007;46(8):623–644. doi:10.2165/00003088-200746080-00001
8. Hung SI, Chung W-H, Liou L-B, et al. HLA-B*5801 allele as a genetic marker for severe cutaneous adverse reactions caused by allopurinol. *Proc Natl Acad Sci U S A.* 2005;102(11):4134–4139. doi:10.1073/pnas.0409500102
9. Sukasem C, Jantararungtong T, Kuntawong P, et al. HLA-B (*) 58:01 for allopurinol-induced cutaneous adverse drug reactions: implication for clinical interpretation in Thailand. *Front Pharmacol.* 2016;7:186. doi:10.3389/fphar.2016.00186
10. Wu R, Cheng Y-J, Zhu -L-L, et al. Impact of HLA-B*58:01 allele and allopurinol-induced cutaneous adverse drug reactions: evidence from 21 pharmacogenetic studies. *Oncotarget.* 2016;7(49):81870–81879. doi:10.18632/oncotarget.13250
11. Kang HR, Jee YK, Kim Y-S, et al. Positive and negative associations of HLA class I alleles with allopurinol-induced SCARs in Koreans. *Pharmacogenet Genomics.* 2011;21(5):303–307. doi:10.1097/FPC.0b013e32834282b8
12. White WB, Saag KG, Becker MA, et al. Cardiovascular safety of febuxostat or allopurinol in patients with gout. *N Engl J Med.* 2018;378(13):1200–1210. doi:10.1056/NEJMoa1710895
13. Yoon S, Lee H, Jang I-J, et al. Pharmacokinetics, pharmacodynamics, and tolerability of LC350189, a novel xanthine oxidase inhibitor, in healthy subjects. *Drug Des Devel Ther.* 2015;9:5033–5049. doi:10.2147/DDDT.S86884
14. Lin S, Lou Y, Hao R, et al. A single-dose, randomized, open-label, four-period, crossover equivalence trial comparing the clinical similarity of the proposed biosimilar rupatadine fumarate to reference Wystemm[®] in healthy Chinese subjects. *Front Pharmacol.* 2024;15:1328142. doi:10.3389/fphar.2024.1328142
15. Shang K, Ge C, Zhang Y, et al. An evaluation of sex-specific pharmacokinetics and bioavailability of kokusaginine: an in vitro and in vivo investigation. *Pharmaceuticals.* 2024;17(8):1053. doi:10.3390/ph17081053
16. Li W, Wu J, Zhang J, et al. Puerarin-loaded PEG-PE micelles with enhanced anti-apoptotic effect and better pharmacokinetic profile. *Drug Deliv.* 2018;25(1):827–837. doi:10.1080/10717544.2018.1455763
17. Murrell GA, Rapeport WG. Clinical pharmacokinetics of allopurinol. *Clin Pharmacokinet.* 1986;11(5):343–353. doi:10.2165/00003088-198611050-00001
18. Dalbeth N, Stamp L. Allopurinol dosing in renal impairment: walking the tightrope between adequate urate lowering and adverse events. *Semin Dial.* 2007;20(5):391–395. doi:10.1111/j.1525-139X.2007.00270.x
19. Kotozaki Y, Satoh M, Nasu T, et al. Human plasma xanthine oxidoreductase activity in cardiovascular disease: evidence from a population-based study. *Biomedicines.* 2023;11(3):754. doi:10.3390/biomedicines11030754
20. Li H, Zhang C, Fan R, et al. The effects of Chuanxiong on the pharmacokinetics of warfarin in rats after biliary drainage. *J Ethnopharmacol.* 2016;193:117–124. doi:10.1016/j.jep.2016.08.005
21. Lou Y, Song F, Cheng M, et al. Effects of the CYP3A inhibitors, voriconazole, itraconazole, and fluconazole on the pharmacokinetics of osimertinib in rats. *PeerJ.* 2023;11:e15844. doi:10.7717/peerj.15844

Drug Design, Development and Therapy

Dovepress
Taylor & Francis Group

Publish your work in this journal

Drug Design, Development and Therapy is an international, peer-reviewed open-access journal that spans the spectrum of drug design and development through to clinical applications. Clinical outcomes, patient safety, and programs for the development and effective, safe, and sustained use of medicines are a feature of the journal, which has also been accepted for indexing on PubMed Central. The manuscript management system is completely online and includes a very quick and fair peer-review system, which is all easy to use. Visit <http://www.dovepress.com/testimonials.php> to read real quotes from published authors.

Submit your manuscript here: <https://www.dovepress.com/drug-design-development-and-therapy-journal>